Borah D, Cummins C, Rasappa S, Watson SMD, Pike AR, Horrocks BR, Fulton DA, Houlton A, Liontos G, Ntetsikas K, Avgeropoulos A, Morris MA.

Nanoscale silicon substrate patterns from self-assembly of cylinder forming poly (styrene)-block-poly(dimethylsiloxane) block copolymer on silane functionalized surfaces.

***Nanotechnology* 2017, 28(4)**

Nanoscale Silicon Substrate Patterns From Self-assembly of Cylinder Forming Poly(styrene)-*block*-poly(dimethylsiloxane) Block Copolymer on Silane Functionalized Surfaces

Dipu Borah,[1,2,3*] Cian Cummins,[3] Sozaraj Rasappa,[1,3] Scott M. D. Watson,[4] Andrew R. Pike,[4] Benjamin R. Horrocks,[4] David A. Fulton,[4] Andrew Houlton,[4] George Liontos,[5] Konstantinos Ntetsikas,[5] Apostolos Avgeropoulos,[5] and Michael A. Morris[1,2,3*]

[1] Department of Chemistry, University College Cork, Cork, Ireland

[2] Tyndall National Institute, Lee Maltings, Prospect Row, Cork, Ireland

[3] AMBER, Centre for Research on Adaptive Nanostructures and Nanodevices (CRANN), Trinity College Dublin, Dublin 2, Ireland

[4] Chemical Nanoscience Laboratory, School of Chemistry, Newcastle University, Newcastle upon Tyne, NE1 7RU, United Kingdom

[5] Department of Materials Science and Engineering, University of Ioannina, University Campus-Dourouti, 45110 Ioannina, Greece

*Corresponding author:

Email: borahd@tcd.ie (Dipu Borah) and morrism2@tcd.ie (Michael A Morris)

Abstract

Poly(styrene)-*block*-poly(dimethylsiloxane) (PS-*b*-PDMS) is an excellent block copolymer (BCP) system for self-assembly and inorganic template fabrication because of its high Flory-Huggins parameter (χ ~0.26) at room temperature in comparison to other block copolymers, and high selective etch contrast between PS and PDMS block for nanopatterning. In this work, self-assembly in PS-*b*-PDMS BCP is achieved by combining hydroxyl-terminated poly(dimethylsiloxane) (PDMS-OH) brush surfaces with solvent vapor annealing. As an alternative to standard brush chemistry, we report a simple method based on the use of surfaces functionalized with silane-based self-assembled monolayers (SAMs). A solution-based approach to SAM formation was adopted in this investigation. The influence of the SAM-modified surfaces upon BCP films was compared with polymer brush-based surfaces. The cylinder forming PS-*b*-PDMS BCP and PDMS-OH polymer brush were synthesized by sequential living anionic polymerization. It was observed that silane SAMs provided the appropriate surface chemistry which, when combined with solvent annealing, led to microphase segregation in the BCP. It was also demonstrated that orientation of the PDMS cylinders may be controlled by judicious choice of the appropriate silane. The PDMS patterns were successfully used as an on-chip etch mask to transfer the BCP pattern to underlying silicon substrate with sub-25 nm silicon nanoscale features. This alternative SAM/BCP approach to nanopattern formation shows promising results, pertinent in the field of nanotechnology, and with much potential for application, such as in the fabrication of nanoimprint lithography stamps, nanofluidic devices or in narrow and multilevel interconnected lines.

KEYWORDS: self-assembly; block copolymer; self-assembled monolayer; solvent vapor anneal; pattern transfer

1. Introduction

Semiconductor device performance has been subject to continuing improvements over the years (*i.e.* Moore's Law [1]), largely due to a reduction of device dimensions as a consequence of improving resolution limits of UV lithographic processes used in device fabrication. Advancements in such technology have now seen device fabrication possible with feature sizes approaching sub-10 nm resolution [2]. However, in addition to the continuing goal of realizing further reductions in device dimensions, additional challenges are also presented such as achieving device fabrication with ultra-high precision (structural regularity and position relative to defined locations and directions), for the manufacture of logic and memory circuitry [3].

Various alternative "top-down" methodologies to device fabrication are currently being examined, which might allow silicon-based devices to reach their ultimate feature size and performance [3],[4],[5],[6],[7]. However, in parallel to the physical engineering of substrate features, "bottom-up" approaches, based on hierarchical self-assembly of structures ranging from molecular building blocks through to nanoparticles and macromolecular structures, are also the subject of intense research [8]. Both approaches are recognized to present different advantages and drawbacks to device fabrication. In "top-down" methodologies for example, further progress is critically related to several issues including source design, material interactions and thermal management [9],[10]. On the other hand, it is highly challenging to achieve long-range translational order and robustness of systems fabricated with "bottom-up" approaches [11],[12],[13],[14].

Block copolymer (BCP) lithography is a "bottom-up" process that relies upon microphase separation within thin films of the BCP. This approach holds much promise for the fabrication of nanopatterns with sub-10 nm scale features, in addition to offering potential for integration into existing manufacturing processes [15],[16],[17]. BCP nanolithographic methods have already been demonstrated for application in the fabrication of nanowires [18], magnetic arrays [19], and nanoporous membranes [20]. BCP self-assembly offers significant control over pattern dimension, orientation and structure through the variation of the molecular weight (Mw), relative volume fraction (ϕ) and the segmental interaction parameter (χ). High χ BCPs possessing a low Mw enable access to small feature sizes as well as lower line edge roughness that are pertinent for nanolithographic patterning [17]. BCPs allow the formation of a number of different morphological structures *viz.*, lamellar, cylindrical, spherical, gyroidal, [21].

BCPs containing inorganic components, *e.g.* poly(dimethylsiloxane) (PDMS), are particularly useful because they can be processed to directly yield an oxide nanostructure without the need for any selective polymer chemistry [22],[23],[24],[25],[26],[27]. The PS-*b*-PDMS BCP system has particular relevance because of its high Flory-Huggins parameter (χ ~0.26) [28]. However, the two major issues that arise in the PS-*b*-PDMS system *viz.*, (i) strong surface dewetting due to the high hydrophobicity of the BCPs, leading to multilayer formation, and (ii) poor control over microdomain orientation, particularly for definition of parallel versus vertical cylinder alignment. A surface pre-treatment with a hydroxyl-terminated poly(dimethylsiloxane) (PDMS-OH) homopolymer brush has typically been used previously to overcome these limitation [24]. However, the use of a PDMS-OH brush can present further problems for pattern transfer into the underlying substrate. For example, the PDMS-OH brush modification produces a PDMS layer at the substrate-polymer (BCP) interface, which effectively increases the thickness of the passive silica layer at the substrate surface. The presence of this layer subsequently impedes the effectiveness of any selective Si:SiO_2 etch chemistry used for pattern transfer [29]. Despite such drawbacks being recognized to arise with the use of PDMS-OH brushes, alternative approaches to substrate functionalization which similarly facilitate improved wetting behaviour of the BCP films and thin PDMS layer formation at the interface, remain scarce [22],[30],[31],[32]. One should note a recent report on the use of a PS-*block*-poly(dimethylsiloxane-*random*-vinylmethylsiloxane) (PS-*b*-P(DMS-*r*-VMS)) BCP that was processed on a PMMA-OH brush without any dewetting issues to form excellent line patterns after rapid thermal annealing [33].

Herein, we report the functionalization of substrate surfaces with self-assembled monolayers (SAMs) of silane-based compounds, upon which high levels of wetting and orientation control were afforded over a cylindrical phase forming PS-*b*-PDMS BCP system. The effectiveness of the SAM approach to surface modification was compared to the more conventional PDMS-OH polymer brush systems that have typically been used in conjunction with this BCP. The potential utility of this SAM-based approach has also been highlighted through demonstrating that PS-*b*-PDMS nanopatterns can be used to create nanoscale silicon patterns with excellent uniformity.

2. EXPERIMENTAL SECTION

2.1. Polymer Synthesis

The PS-*b*-PDMS BCP was synthesized by sequential living anionic polymerization of styrene and hexamethylcyclotrisiloxane (D_3), employing high vacuum techniques as described in the ***Supporting Information***. The number average molecular weights (M_n) per block and polydispersity index (M_w/M_n) of the BCP were determined using Membrane Osmometry (MO) and Size Exclusion Chromatography (SEC) experiments leading to values: M_n^{PS}= 53.0 kg mol^{-1}, M_n^{PDMS}= 17.0 kg mol^{-1}, and M_w/M_n= 1.07. The volume fraction (ϕ_{ps}) of PS in the BCP was calculated by ^{1}H-nuclear magnetic resonance (NMR) spectroscopy equal to 0.72. The hydroxyl-terminated PDMS (PDMS-OH) polymer brush was synthesized by living anionic polymerization of hexamethylcyclotrisiloxane (D_3) with sec-BuLi as initiator, end capped with 1-2 monomeric units of ethylene oxide (EO) in pyridine and terminated with methanol (MeOH). The number average molecular weight (M_n) and polydispersity (M_w/M_n) of the PDMS-OH were determined by MO and SEC techniques equal to: M_n^{PDMS}= 5.5 kg mol^{-1} and M_w/M_n= 1.06, respectively. The molecular characterization results from SEC, MO and ^{1}H-NMR for the two polymers (BCP and PDMS-OH) indicate molecular and compositional homogeneity. The potential for microphase separation of the BCP is indicated by differential scanning calorimetry (DSC) and the results exhibit two distinctive glass transition temperatures: T_{g1}= ~150.74 K (-122.41 ^{o}C) and T_{g2}= ~375.35 K (102.02 ^{o}C), corresponding to non-miscible PDMS and PS macromolecular chains, respectively. The details of molecular characterization are available in the Supporting Information.

2.2. Surface Functionalization with PDMS-OH Brush

Silicon <100> substrates (B doped, *p*-type, thickness 525 ± 25 μm, resistivity 1-10 ohm-cm) with a native oxide layer were cut into ~1.0 cm^2 pieces, rinsed in acetone (≥ 99.8 %) and washed with NANOpure® water. The substrates were then washed in a 0.1 % (m/v) dodecyl sodium salt solution at 343 K for 20 min, followed by thorough rinsing with NANOpure® water and sonicating in NANOpure® water for 10 min. Piranha treatment (*1:4* v/v 30% H_2O_2:H_2SO_4) *(Caution! Piranha solution should be handled with extreme care; it is a strong oxidant and reacts violently with many organic materials. It also presents an explosion danger)* of the substrates was subsequently carried out at 353 K for 45 min, followed by rinsing with copious amounts of NANOpure® water, and dried under flowing N_2 gas followed by baking for 5 min at 373 K in an ambient atmosphere to remove any residual water. A solution of hydroxyl-

terminated PDMS-OH of 1.0 wt % in toluene was spin-coated (P6700 Series Spin-coater, Speciality Coating Systems, Inc., USA) onto substrates at 3000 rpm for 30 s. Samples were annealed in a vacuum oven (Townson & Mercer EV018) at 443 K under vacuum (~ *1 Pa*) for 6 h. This allows the end-functional hydroxyl groups of the polymer brush to diffuse through the deposited brush layer and react with the silicon native oxide layer, resulting in polymer chain brushes covalently anchored to the substrate. Unbound PDMS-OH polymer was removed by ultrasonication (Cole-Palmer 8891 sonicator) and rinsing in toluene, followed by drying for 30 min at 333 K in an ambient atmosphere to remove any residual toluene.

2.3. Surface Functionalization with Silane SAMs

SAMs of octadecylsiloxane (OTS) or octadecyl(dimethyl)siloxane (ODS) were prepared upon the piranha activated silicon substrates (*see above*) through treatment in a 1.0 mM solutions of octadecyltrichlorosilane or octadecyl(dimethyl)chlorosilane in toluene, for 24 h, respectively. The silane solutions and subsequent deposition onto silicon substrates were carried out in a glove box. The substrates were subsequently sonicated successively in 3 volumes of toluene, for 15 min in each, followed by sonication in 3 successive volumes of hexane, for 15 min in each.

2.4. BCP Thin Films Preparation and Solvent Anneal

Thin films of PS-*b*-PDMS were prepared by depositing a dilute solution (1.0 wt. %) of the BCP in toluene onto functionalized silicon substrates by spin coating (3200 rpm and 30 s). As-cast thin films were solvent annealed in glass jars under a saturated toluene environment at room temperature (~288 K) for 3 h. Samples were removed from the glass jars after the desired anneal time and the trapped solvent allowed to evaporate at ambient conditions.

2.5. Plasma Etching of PS-*b*-PDMS Films and Pattern Transfer

Following BCP film formation, atomic force microscopy cannot readily identify the microphase separated structure of the film due to the presence of a surface wetting layer of PDMS. This is required to be removed in order to reveal the BCP arrangement [22],[27],[34],[35],[36]. To achieve this, an etch process (ETCH1) was developed. This etch was one component of a multi-step process that allowed pattern transfer to the substrate. Solvent annealed PS-*b*-PDMS films were first treated with a CF_4 (15 sccm) plasma for 5 s with an inductively coupled plasma (ICP) and reactive ion etching (RIE) at powers of 400 W and 30 W, respectively, at 2.0 Pa, with a helium backside cooling pressure of 1333.2 Pa to remove any surface PDMS layer. This was followed by an O_2 (30 sccm) plasma for 10 s with an ICP (1200 W) and RIE (30 W) at 2.0 Pa,

with a helium backside cooling pressure of 666.6 Pa. These steps follow a similar methodology developed by Jung and Ross [27]. The process removes the PS component and generates an oxidized form of PDMS on the substrate.

The oxidized PDMS cylinders were subsequently used as an etch mask for pattern transfer (*i.e.*, ETCH2). This second processing methodology involves a CHF_3 (80 sccm) and Ar (30 sccm) plasma etch for 5 s with an ICP (400 W) and RIE (30 W) at 1.6 Pa to remove any residual PDMS wetting layer at the substrate surface. This milder etch treatment is critical and required careful optimization. It is used to remove passive silica and any PDMS components at the silicon substrate surface without removing the 'etch mask' formed by the oxidized PDMS cylinders. This process was followed by a selective silicon etch using CHF_3 (80 sccm) and SF_6 (15 sccm) gases for 15 s with an ICP (1200 W) and RIE (30 W) at 2.0 Pa, with a helium backside cooling pressure of 1333.2 Pa to transfer the patterns into the underlying substrate. The polymer remaining after pattern transfer was removed by ETCH3. The residual oxidized PDMS cylinders were removed by a 10 s silica (SiO_2) etch based on CHF_3 (80 sccm) and Ar (15 sccm) gases with an ICP (1200 W) and RIE (40 W), at 2.0 Pa with a helium backside cooling pressure of 1333.2 Pa. This is followed by a 5 s O_2 (30 sccm) etch to remove the residual PS matrix underneath with an ICP (2000 W) and RIE (100 W) at 1.3 Pa, with a helium backside cooling pressure of 666.6 Pa. All the etching processes were accomplished in an OIPT Plasmalab System100 ICP180 etch tool.

The details of the process flow depicting surface functionalization on silicon substrate and the etch steps to fabricate nanoscale silicon patterns are shown in **Scheme 1**.

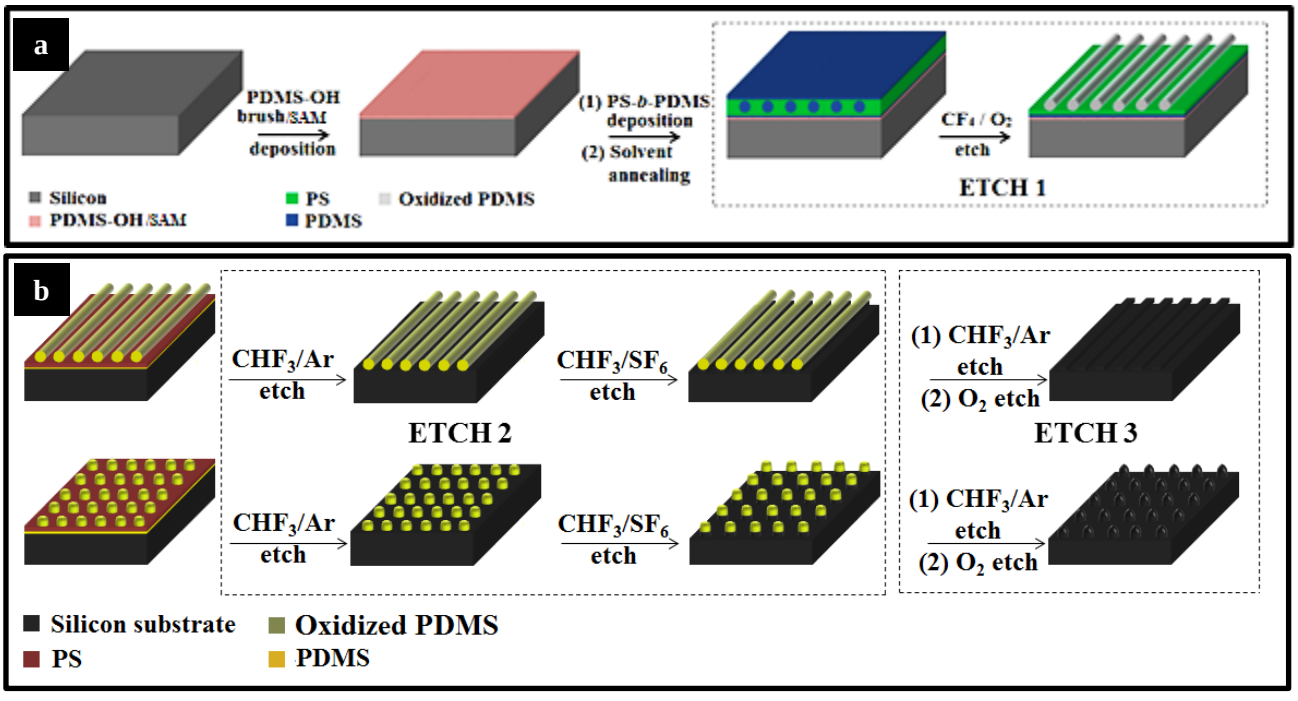

Scheme 1. (a) Schematic of the process flow depicting surface functionalization of silicon substrate, PS-*b*-PDMS BCP self-assembly, and sequential CF_4 and O_2 plasma etching (**ETCH1**) to remove PDMS surface wetting layer and PS matrix (partially). **(b)** Scheme demonstrating details of the pattern transfer process following **ETCH2** and **ETCH3** to fabricate silicon nanscale features on substrate surface. See text for details.

2.6. Characterization of Materials

Contact Angle: Static contact angles of NANOpure® water were measured on SAM/PDMS-OH functionalized silicon substrates at ambient temperature using a CAM101 goniometer system (KSV Instruments Ltd.). Contact angles were again measured on the opposite edges of at least three drops and averaged.

Film Thickness: Film thickness was determined by spectroscopic ellipsometry (Plasmos SD2000 Ellipsometer) at a fixed incidence angle of 70^o. For each sample an average of five measurements, carried out at different locations on a sample surface, was reported as the film thickness. A two layer model (SiO_2 + polymer brush/SAM) for polymer brush/SAM and a three layer model (SiO_2 + polymer brush/SAM + BCP) for total BCP film were used to simulate experimental data.

Atomic Force Microscopy (AFM): Scanning probe microscopy measurements (topography and phase data) of the SAM-modified silicon substrates were acquired using both a Multimode Nanoscope IIIa and Dimension Nanoscope V system (Veeco Instruments Inc., Metrology Group) equipped with Nanscope version 5.12b36 and 7.00b19 software, respectively. Data was acquired using TESP, n-doped silicon cantilevers, f_0 = 230 - 280 kHz, spring constant = 20 - 80 N m^{-1}) (Veeco Instruments Inc., Digital Instruments) and Tap300Al-G (silicon cantilevers, f_0 = 200 - 400 kHz, spring constant = 20 - 75 N m^{-1}) (BudgetSensors) model AFM probes. An isolation table and acoustic enclosure was used to reduce vibrational noise (Veeco Inc., Metrology Group).

Scanning Electron Microscope (SEM): SEM images were obtained by a high resolution (< 1 nm) Field Emission Zeiss Ultra Plus-SEM with a Gemini® column operating at an accelerating voltage of 5 kV. The SEM images were processed using ImageJ software. For FIB preparation of lamellae, an FEI Strata 235-Focused Ion Beam (FIB) tool was used. E-beam platinum was

deposited at the substrate followed by the ion-beam deposited platinum. Milling and polishing of the samples were carried out at the lower aperture size and the specimen was imaged under the higher resolution Zeiss Ultra Plus-SEM.

3. RESULTS AND DISCUSSION

3.1. Effect of PDMS-OH Brush on BCP Self-assembly

The PS-*b*-PDMS BCP used in the study possess a total molecular weight of 70 kg mol^{-1} and a volume fraction of the PS block of 72%. As mentioned earlier and in the *Supporting Information*, this BCP shows a thermodynamic equilibrium structure of cylindrical PDMS domains in a PS matrix. In order to promote parallel alignment of PDMS cylinders in cylinder-forming PS-*b*-PDMS BCP, the substrate are commonly functionalized with a hydroxyl-terminated PDMS homopolymer brush [22],[27],[34],[35],[36]. This approach was employed in the studies described here, with silicon substrates functionalized with a PDMS-OH brush layer ~ 4.3 nm in thickness, as determined by ellipsometry. The PDMS-OH brush layer facilitates self-assembly in PS-*b*-PDMS with a wetting PDMS layer on the surface and bottom of the patterns, similar to previously reported examples [22],[27],[34],[35],[36]. An etch process was required to remove this surface PDMS wetting layer and allow the underlying BCP arrangement to be observed. This was achieved using an etch methodology previously reported by Jung and Ross [27]. This series of etching protocols not only removes the surface PDMS wetting layer, but also results in partial removal of the PS component of the BCP film and generates an oxidized form of PDMS cylinders on the substrate. Figure 1 shows the pattern formed by the PS-*b*-PDMS BCP on a PDMS-OH brush-functionalized silicon substrate as revealed by SEM of the etched film. Although it has been observed by SEM that the BCP film effectively wets the entire substrate surface when a polymer brush layer is present, the film is found to dewet upon subsequent solvent vapor annealing. Dewetting is a major issue with high χ PS-*b*-PDMS systems, leading to poor substrate coverage (typically ~ 60 % of the overall surface area), multilayer pattern formation, lower correlation length of PDMS cylinders, and macroscopic defects such as disclinations and dislocations. The optical image in Figure 1 reveals significant levels of dewetting of the BCP film after solvent vapor annealing. The mean PDMS L_0 and line width <d> are found to be ~63.5 nm and ~31.8 nm, respectively.

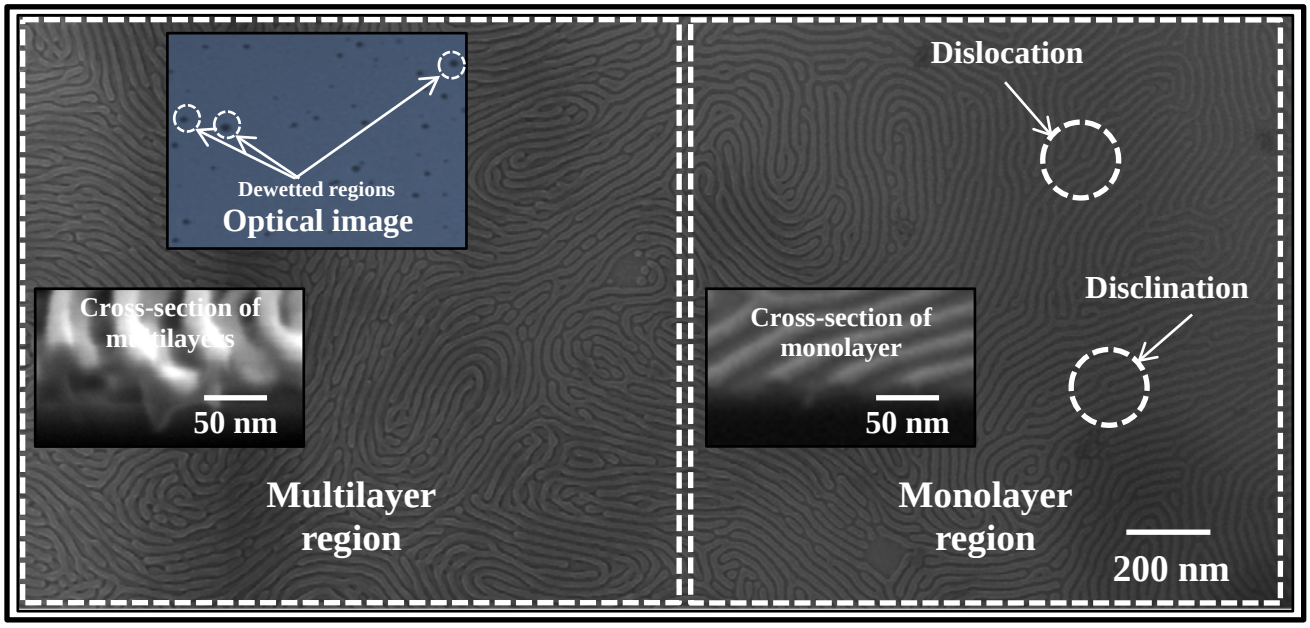

Figure 1. Top-down SEM image of PS-*b*-PDMS derived structures formed at silicon substrate anchored with PDMS-OH polymer brush after sequential CF_4 and O_2 etches. Insets, are cross-section SEM images of multilayers and monolayer of PDMS cylinders, and an AFM optical image of the BCP film after solvent vapor annealing.

3.2. Substrate Functionalization with Silanes

Substrate functionalization based around self-assembled monolayers (SAMs) of silane compounds is explored here as an alternative to the more conventional PDMS-OH polymer brush method previously discussed. The use of silane SAMs in place of polymer brushes offer several advantages including their lower cost, and ease of preparation in comparison to the more tedious processes involved in polymer brush grafting. In addition, the use of silane SAMs may avoid the formation of thick PDMS wetting layers at the polymer-substrate interface, which typically results when using PDMS polymer brush surfaces due to the favorable PDMS (brush) - PDMS (BCP) interactions [34],[35],[36].

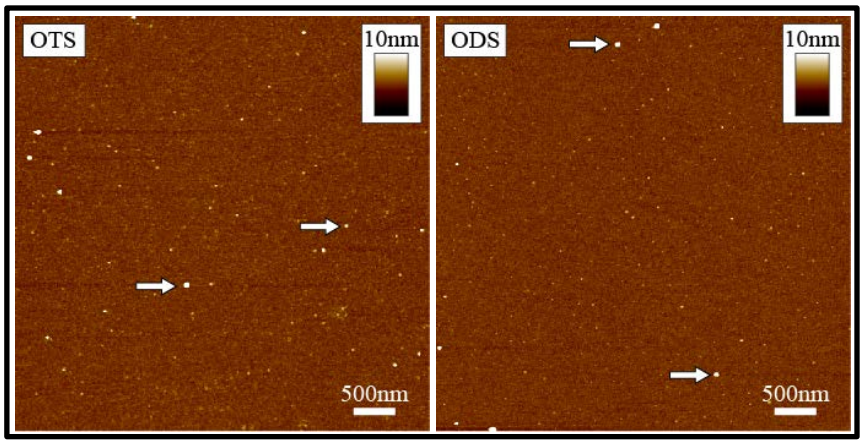

Figure 2. Tapping mode AFM topography images of silicon substrates modified with OTS (left) and ODS (right) SAMs *via* exposure of the silicon substrate to a solution of the appropriate silane compound for a period of 24 h.

Herein, we demonstrate the use of two types of silanes *viz.*, octadecyl(dimethyl)chlorosilane (Cl-ODS) and octadecyltrichlorosilane (Cl_3-OTS) for SAM modification of silicon substrates using a solution-based approach. AFM imaging was carried out to evaluate the surface quality of the SAMs prepared. Figure 2 shows AFM height images of both types of SAM-modified silicon substrates prepared. The images reveal good surface uniformity irrespective of the silane used for SAM formation, with rms roughness values over a 5 x 5 μm^2 regions determined to be 0.36 nm (stand. dev. = 0.10 nm) and 0.32 nm (stand. dev. = 0.06 nm) for the ODS and OTS SAMs, respectively. For comparison, AFM scans (figure omitted for brevity) were carried out at various locations of the substrate (prior to SAM deposition) revealed the rms roughness to be in the range of 0.10-0.15 nm (stand. dev. = 0.04 nm). It is also noted that evidence of particulate contamination can be seen across the SAM surfaces, see Figure 2 (white arrows). The origin of these particulates is likely to be the formation of aggregates of the silane material in solution which physisorb to the SAM surface. The Si-Cl bonds in the “headgroups” of such silane molecules are susceptible to hydrolysis, which may lead to the formation of Si–O–Si linkages between silane molecules [39, 40]. Particularly in the case of Cl_3-OTS which contains three Si–Cl bonds, the presence of trace amounts of water in the silane solution will result in some hydrolytic polymerization of the silane, resulting in the formation of aggregates which physisorb on the SAM surface. However, the presence of these particulates on the SAM surface are not seen to have a detrimental impact upon the BCP films deposited on top, with excellent BCP film coverage observed. The uniform coverage of the BCP across the substrate support also provides

supporting evidence that the SAM architectures are highly regular, and result in homogenous functionalization of the silicon substrate.

Table 1. Water Contact Angle and Film Thickness Data of Polymer Brush, Silane SAMs and BCP Films on Silicon Substrates

film type	silane or polymer concentration, wt. %	conditions of film preparation	film thickness, nm	contact angle, ^{o}
silicon substrate	-	as-received	-	42.7
silicon substrate	-	piranha activation	-	28.3
PDMS-OH brush layer	1.0	annealed and cleaned	4.3	109.4
ODS SAM	-	24 h solution preparation	-	94.3
OTS SAM	-	24 h solution preparation	-	113.8
PDMS-OH + BCP	1.0	as-cast	54.4	-
ODS SAM + BCP	1.0	as-cast	48.7	-
OTS SAM + BCP	1.0	as-cast	50.5	-

The effect of the two types of silane functionalization on the substrate wetting properties was characterized by static contact angle measurements, using high purity water as the probe liquid, and compared with both unmodified and PDMS-OH modified silicon surfaces. Water contact angles can qualitatively portray the density of attached silane molecules on a SAM-modified surface. Data presented in Table 1 reveals that the contact angle of as-received silicon substrate was ~ 43^{o} (mean = 42.7°, stand. dev. = 0.5) which is reduced significantly to ~ 28^{o} (mean = 28.3°, stand. dev. = 0.6) upon "activation" with piranha solution (H_2O_2/H_2SO_4). This is consistent with the piranha solution generating an increased number of Si–OH groups at the silicon surface, making it more hydrophilic, *i.e.*, water contact angles are reduced. Water contact angles measure upon the PDMS-OH functionalized substrates were determined to be 109^{o} (mean = 109.4°, stand. dev. = 0.3), *i.e.*, the surface is hydrophobic. The water contact angles recorded upon the ODS and

OTS modified silicon substrates were determined to be ~ 94^{o} (mean = 94.3°, stand. dev. = 0.7°) and ~ 114^{o} (mean = 113.8°, stand. dev. = 0.4), respectively. In the case of the OTS SAMs, this proves to be consistent with typical literature values for well-ordered, densely-packed OTS SAMs [37]. It should also be noted that this value is similar to the water contact angles measured upon the PDMS-OH brush surfaces, indicating the OTS SAM will provide similar conditions as the PDMS-OH brush surfaces for PS-*b*-PDMS self-assembly. In the case of the ODS SAMs, the lower contact angle values observed can be explained by the presence of the two methyl groups attached to the "Si" in the "headgroups" of the SAMs constituent silane molecules. The presence of these groups sterically hinder the packing of the silane molecules, leading to a less densely packed monolayer in comparison to the OTS SAMs. The contact angles associated with the ODS SAMs also represent a surface that is less hydrophobic in comparison to the PDMS-OH brush surfaces.

3.3 BCP Self-assembly on ODS/OTS Functionalized Surfaces

Self-assembly of PS-*b*-PDMS BCP was studied on planar silicon substrates modified with silane SAMs by solvent annealing of the BCP film. SEM images of the resulting BCP arrangements on the respective SAM-modified substrates are shown in Figure 3. SAM modification of the silicon substrates was found to result in substantial improvements in the wetting behavior of the BCP compared to the use of PDMS-OH brush surfaces, with > 90 % coverage observed, along with uniform film thickness. In comparison, the PDMS-OH polymer surfaces result in BCP surface coverages of ~ 60 %, *i.e.* significantly more dewetting of the BCP takes place due to high hydrophobicity of the brush surface.

The low resolution large area SEM images in Figure 3 for ODS and OTS coated substrates provide direct evidence of superior BCP coverage. Further, the optical images shown in figure 3 reveal that unlike the BCP film on PDMS-OH brush coated substrates, the level of dewetting is minimized when using silane functionalized substrates. Figure 3 shows that the BCP forms *in-plane* PDMS cylindrical patterns oriented parallel to the substrate surface in a PS matrix when on an OTS SAM surface. However, upon the ODS SAM surface, it shows a mixed morphology of *in-plane* cylindrical and *out-of-plane* spherical PDMS structures. Thus the results reveal the existence of two kinds of self-assembly morphologies depending on the silane type. A closer

look at the BCP patterns on the ODS SAM surface reveals the formation of a variety of line and sphere morphologies which includes hexagonal sphere patterns, hexagonally packed cylinders and mixed overlying cylinders on sphere patterns. These morphologies may be the result of variation of BCP film thickness on ODS surface after solvent vapor annealing. One must also consider that the resulting morphologies observed on ODS material are due to non-ideal surface wetting of the BCP since such mixed features were not observed on PDMS-OH or OTS SAM layers after identical solvent vapor annealing conditions. The mean PDMS L_0 and line width <d> are found to be ~63.5 nm and ~31.8 nm, respectively, similar to the PDMS-OH brush coated surfaces. For the spherical morphology, the periodicity and the PDMS sphere dimension have been found to be ~79.4 nm and ~35.2 nm, respectively. Formation of a spherical morphology in the thin film could be due to the constraints of the film thickness or solvent effects during the casting/anneal process [37]. Here it should be noted that a PDMS cylindrical pattern in PS matrix is the thermodynamic equilibrium structure for this BCP. Hsieh *et al* [38] observed a similar spherical morphology for a cylinder- forming PS-*b*-PDMS and concluded that formation of the spherical structure is principally driven by solvent effects during the formation process. When using toluene (solubility parameter, $\delta_{Toluene}$ ~18.2 $(J\ cm^{-3})^{1/2}$) as the solvent during the solvent anneal process for example, the toluene is a better solvent for PS (δ_{PS} ~18.6 $(J\ cm^{-3})^{1/2}$) in comparison to PDMS (δ_{PDMS} ~15.4 $(J\ cm^{-3})^{1/2}$), and hence preferentially swells the PS blocks, driving the formation of PS sphere structures during the casting/annealing process [39],[40]. It should be noted that the PS volume fraction gradually decreases toward its original bulk state composition during solvent evaporation and at the same time the PS glass transition temperature gradually increases with the decrease in solvent concentration. This results in freezing the phase structure as the solvent swollen PS glass transition temperature (T_g^{PS}) reaches ambient temperature [41], and forces the system to deviate from adopting the thermodynamic equilibrium lamellar morphology. It can be seen from the SEM data (figure 3) that despite the improvement in terms of the BCP wetting (compared to the PDMS-OH brush surfaces), the *in-plane* PDMS cylinders have similar degree of alignment and correlation lengths in both ODS and OTS surfaces. The disordered structures observed in ODS surface could be the result of the strong interaction between the minority PDMS block and the native SiO_2 layer on the silicon substrate, and poor diffusivity of PDMS onto ODS surface. It should be noted further that both the SAM and the PDMS block of BCP are silicon containing entities, and therefore, it is highly likely that

the formation of a PDMS wetting layer at the SAM-BCP interface can occur. SEM cross-section analysis proved unsuccessful in identifying the thickness of the PDMS wetting layer and could be due to the presence of a very thin wetting layer at the SAM-BCP interface.

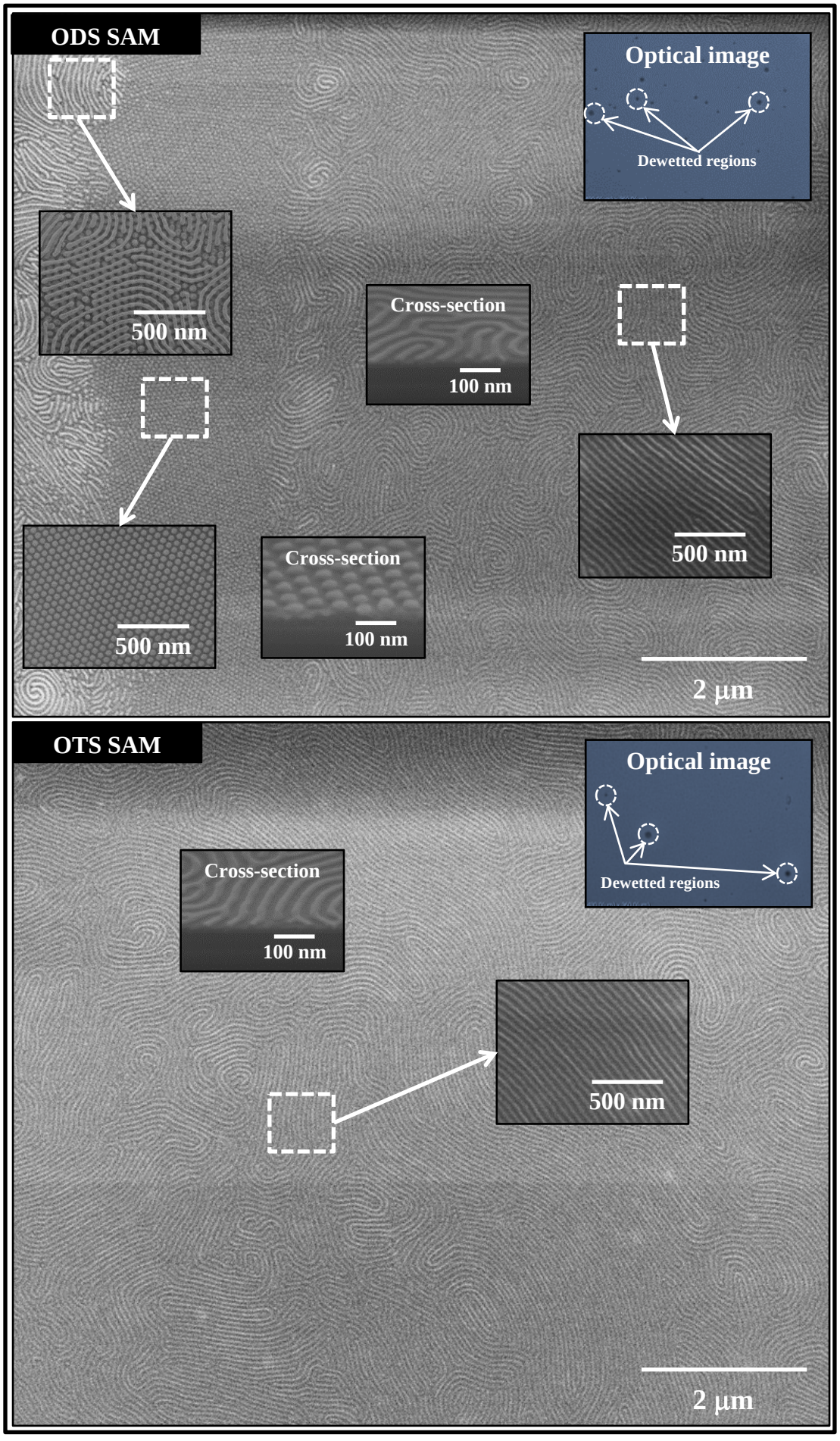
ODS SAM
Optical image
Dewetted regions
500 nm
Cross-section
100 nm
500 nm
Cross-section
100 nm
500 nm
2 μm
OTS SAM
Optical image
Dewetted regions
Cross-section
100 nm
500 nm
2 μm

Figure 3. Large area low-resolution top-down SEM images of PS-*b*-PDMS derived structures formed at silicon substrates functionalized with ODS and OTS after sequential CF_4 and O_2 etches. Insets are the high-resolution top-down and cross-section SEM images of specific sections and AFM optical images of the BCP films after solvent anneal.

3.3. Pattern Transfer of PDMS Domains to Silicon Substrate

The effectiveness of the cylinder-forming PS-*b*-PDMS system for use as part of a nanofabrication process for generating topographic patterns within silicon substrates was demonstrated by subjecting the BCP films to a plasma etch procedure (ETCH 2). The pattern transfer of PS-*b*-PDMS BCP to the underlying substrate support required a more intricate set of etch protocols compared to other well-established polymer systems *e.g.*, PS-*b*-PMMA [29],[42],[43],[44]. This is because of the complex morphology of the PS-*b*-PDMS BCP self-assembled patterns, *i.e.* the PDMS domains, aligned either parallel or perpendicular to the substrate surface in a PS matrix, are encased underneath wetting PDMS layers, which form at both the polymer (BCP)-air and substrate-polymer (BCP) interface.

The sequential pattern transfer process involves initial sequential CF_4 and O_2 plasma etches to remove the upper wetting PDMS layer and the PS matrix as well as oxidize the PDMS cylinders **(**ETCH1**)**. This results in the PDMS patterns forming silica-type structures which can be subsequently utilized as a hard mask [17],[45],[46]. It should be noted that during the O_2 etch, special care is required in order to minimize the undercut of the PDMS cylinders which can lead to poor quality pattern transfer. The patterns produced by the ETCH1 process were then treated with a CHF_3 and Ar plasma for 5 s in order to remove silica at the substrate surface and expose elemental silicon.

This is a crucial process as an over-etch can compromise the integrity of the silica structures produced from the PDMS patterns. The silicon etch is performed for 20 s with CHF_3 and SF_6 gases to transfer the final BCP-derived pattern into the substrate (ETCH2). This is followed by 10 s CHF_3 and Ar based silica (SiO_2), and 5 s O_2 etches to remove the residual oxidized PDMS cylinders (hard mask), and the PS matrix underneath (ETCH3).

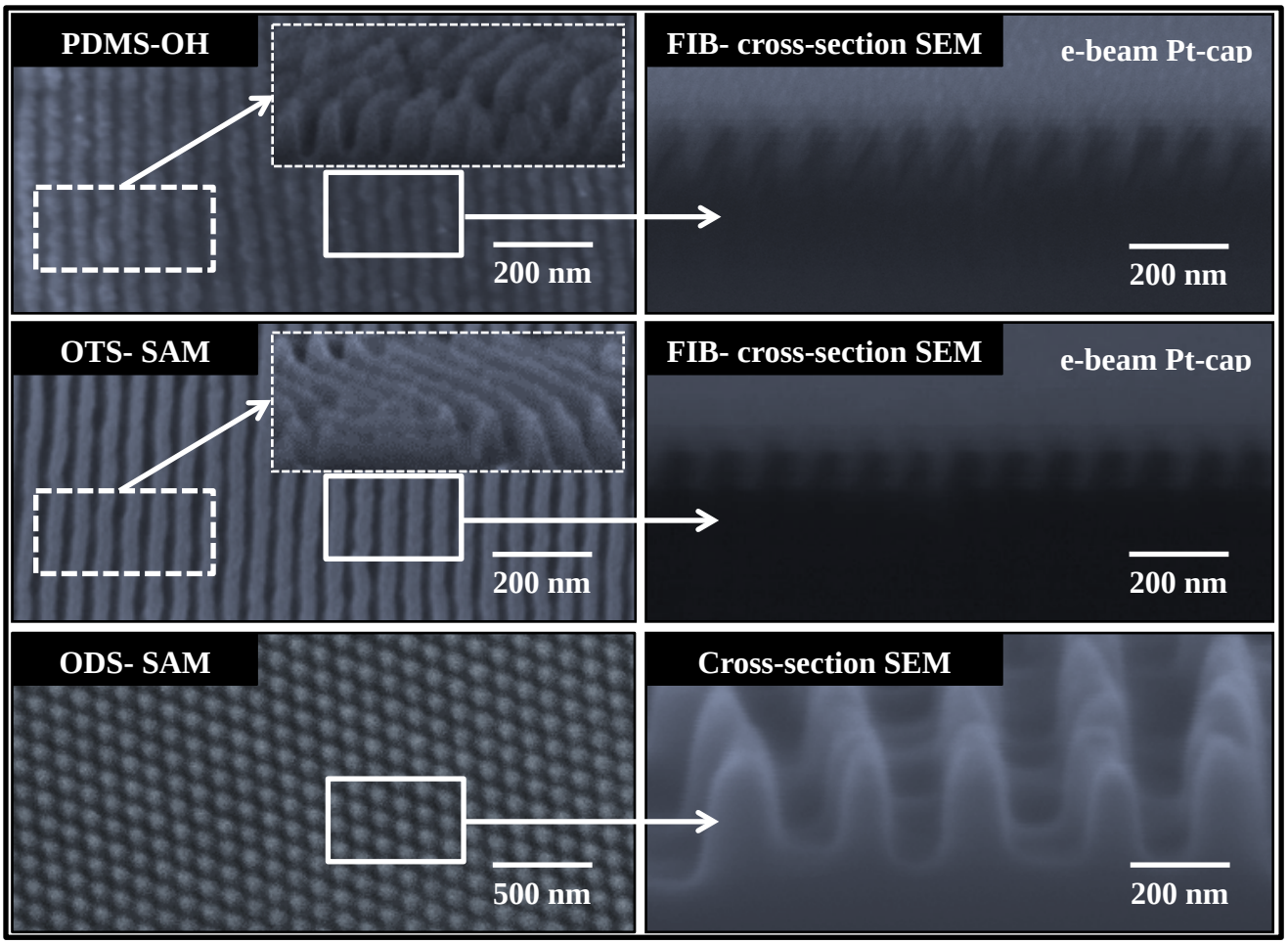

Figure 4. Low resolution top-down and high resolution cross-section SEM images of PDMS patterns transferred to underlying silicon substrates modified with PDMS-OH brush, ODS and OTS SAMs as labelled in the images. The figure includes focused ion beam (FIB) cross-section SEM images of *in-plane* PDMS cylindrical patterns transferred to underlying silicon substrates modified with PDMS-OH brush and OTS SAM.

Figure 4 shows the top-down and cross-section SEM (20^{o} tilted) and FIB-SEM images of the silicon nanowires/nanopillars, on silicon substrates which were precoated with a PDMS-OH brush and silane SAMs, obtained after the sequential etches. The cross-section SEM image shows that the silicon nanowire structures produced have a feature size of ~ 21 nm with a feature height of ~ 45 nm. The FIB cross-section SEM images shown in Figure 4 for the *in-plane* cylindrical patterns gives a more detailed view of the fabricated silicon nanowires. The nanoscale silicon features on the substrate surface are noted to be slightly narrower in width compared to

the initial oxidized PDMS cylinders, attributed to a partly isotropic etch process. It should be noted that the effect of the surface modifying agent (*i.e.*, PDMS-OH and silane) on the silicon nanostructures is difficult to quantify based on the SEM and FIB (top-down and cross-section) images. The spherical PDMS structures obtained on ODS functionalized silicon substrates produced silicon nanopillars upon pattern transfer, with a lateral width and height of ~ 23.4 nm and ~ 48.7 nm, respectively. The silicon nanopillars show good fidelity and aspect ratio (~ 2), though were slightly narrower in width compared to the initial oxidized PDMS spheres due to a partly isotropic etch process as mentioned above. We observed a higher depth profile for the silicon nanopillars due to greater etch resistance of the PDMS spheres, owing to their diameter. This etching method, though complex, proved highly effective for efficient transfer of the PS-*b*-PDMS patterns into the underlying silicon substrate.

4. CONCLUSIONS

We demonstrate here the self-assembly of a synthesized cylinder-forming PS-*b*-PDMS block copolymer on silicon substrates functionalized with silanes as an alternative to standard PDMS-OH polymer brush. The silane functionalized surfaces have shown advantages of tuning the surface properties to improve the wetting property of the BCP and pattern orientation/alignment. While the SAM materials can be prepared in a more facile manner to brush polymers to allow excellent BCP orientation as demonstrated herein, reducing the rather lengthy time for deposition of SAM layers for BCP use deserves further examination. Overall, the effectiveness of the approach is demonstrated by transferring the PDMS cylindrical and spherical patterns to underlying silicon by a complex etching processes developed in our group for generating nanoscale silicon substrate patterns. The method showed promise in guiding self-assembly and subsequent pattern transfer for nanofabrication industry.

Supporting Information

Details of the synthesis and characterization of PS-*b*-PDMS BCP and PDMS-OH polymer brush.

ACKNOWLEDGEMENTS

The authors gratefully acknowledge financial support for this work from the EU FP7 NMP project, LAMAND (grant number 245565) project and Science Foundation Ireland (grant number 09/IN.1/602).

References

[1] Mack C A 2011 Fifty Years of Moore's Law IEEE Transactions on Semiconductor Manufacturing 24 202-7
[2] Freebody M 2011 Preserving Moore's Law Pushes Lithography to its Limits Photonics Spectra 45 45-7
[3] Wissen M, Bogdanski N, Moellenbeck S and Scheer H C 2008 Strategies for hybrid techniques of UV lithography and thermal nanoimprint. In: Mask and Lithography Conference (EMLC), 2008 24th European, pp 1-11
[4] Chung S, Felts J R, Wang D, King W P and De Yoreo J J 2011 Temperature-dependence of ink transport during thermal dip-pen nanolithography Applied Physics Letters 99
[5] Grigorescu A E and Hagen C W 2009 Resists for sub-20-nm electron beam lithography with a focus on HSQ: state of the art Nanotechnology 20 292001
[6] Namatsu H, Watanabe Y, Yamazaki K, Yamaguchi T, Nagase M, Ono Y, Fujiwara A and Horiguchi S 2003 Influence of oxidation temperature on Si-single electron transistor characteristics Journal of Vacuum Science & Technology B 21 2869-73
[7] Hirai Y, Hafizovic S, Matsuzuka N, Korvink J G and Tabata O 2006 Validation of X-ray lithography and development simulation system for moving mask deep X-ray lithography Journal of Microelectromechanical Systems 15 159-68
[8] Hamley I W 2003 Nanotechnology with Soft Materials Angewandte Chemie International Edition 42 1692-712
[9] Biswas A, Bayer I S, Biris A S, Wang T, Dervishi E and Faupel F 2012 Advances in top–down and bottom–up surface nanofabrication: Techniques, applications & future prospects Advances in Colloid and Interface Science 170 2-27
[10] Liddle J A and Gallatin G M 2011 Lithography, metrology and nanomanufacturing Nanoscale 3 2679-88
[11] Kumar P 2010 Directed Self-Assembly: Expectations and Achievements Nanoscale Research Letters 5 1367-76
[12] Katsuhiko A, Jonathan P H, Michael V L, Ajayan V, Richard C and Somobrata A 2008 Challenges and breakthroughs in recent research on self-assembly Science and Technology of Advanced Materials 9 014109
[13] Hawker C J and Russell T P 2005 Block copolymer lithography: Merging "bottom-up" with "top-down" processes MRS Bulletin 30 952-66
[14] Simao C, Tuchapsky D, Khunsin W, Amann A, Morris M A and Sotomayor Torres C M 2014 Defect Analysis and Alignment Quantification of Line Arrays Prepared by Directed Self-assembly of a Block Copolymer Metrology, Inspection, and Process Control for Microlithography XXVIII 9050
[15] Black C T 2007 Polymer Self-Assembly as a Novel Extension to Optical Lithography ACS Nano 1 147-50
[16] Morris M A 2015 Directed self-assembly of block copolymers for nanocircuitry fabrication Microelectronic Engineering 132 207-17
[17] Cummins C, Ghoshal T, Holmes J D and Morris M A 2016 Strategies for Inorganic Incorporation using Neat Block Copolymer Thin Films for Etch Mask Function and Nanotechnological Application Advanced Materials 28 5586-618

[18] Thurn-Albrecht T, Schotter J, Kästle G A, Emley N, Shibauchi T, Krusin-Elbaum L, Guarini K, Black C T, Tuominen M T and Russell T P 2000 Ultrahigh-Density Nanowire Arrays Grown in Self-Assembled Diblock Copolymer Templates Science 290 2126-9
[19] Baruth A, Rodwogin M D, Shankar A, Erickson M J, Hillmyer M A and Leighton C 2011 Non-lift-off Block Copolymer Lithography of 25 nm Magnetic Nanodot Arrays ACS Applied Materials & Interfaces 3 3472-81
[20] Thurn-Albrecht T, Steiner R, DeRouchey J, Stafford C M, Huang E, Bal M, Tuominen M, Hawker C J and Russell T 2000 Nanoscopic templates from oriented block copolymer films Advanced Materials 12 787-91
[21] Hamley I W 2003 Nanostructure fabrication using block copolymers Nanotechnology 14 R39-R54
[22] Hobbs R G, Farrell R A, Bolger C T, Kelly R A, Morris M A, Petkov N and Holmes J D 2012 Selective Sidewall Wetting of Polymer Blocks in Hydrogen Silsesquioxane Directed Self-Assembly of PS-b-PDMS ACS Applied Materials & Interfaces 4 4637-42
[23] Son J G, Chang J-B, Berggren K K and Ross C A 2011 Assembly of Sub-10-nm Block Copolymer Patterns with Mixed Morphology and Period Using Electron Irradiation and Solvent Annealing Nano Letters 11 5079-84
[24] Voet V S D, Pick T E, Park S-M, Moritz M, Hammack A T, Urban J J, Ogletree D F, Olynick D L and Helms B A 2011 Interface Segregating Fluoralkyl-Modified Polymers for High-Fidelity Block Copolymer Nanoimprint Lithography Journal of the American Chemical Society 133 2812-5
[25] Jung Y S, Chang J B, Verploegen E, Berggren K K and Ross C A 2010 A Path to Ultranarrow Patterns Using Self-Assembled Lithography Nano Letters 10 1000-5
[26] Jung Y S and Ross C A 2009 Solvent-Vapor-Induced Tunability of Self-Assembled Block Copolymer Patterns Advanced Materials 21 2540-5
[27] Jung Y S and Ross C A 2007 Orientation-Controlled Self-Assembled Nanolithography Using a Polystyrene−Polydimethylsiloxane Block Copolymer Nano Letters 7 2046-50
[28] Nose T 1995 Coexistence curves of polystyrene/ poly(dimethylsiloxane) blends Polymer 36 2243-8
[29] Borah D, Shaw M T, Rasappa S, Farrell R A, Mahony C O, Faulkner C M, Bosea M, Gleeson P, Holmes J D and Morris M A 2011 Plasma etch technologies for the development of ultra-small feature size transistor devices Journal of Physics D: Applied Physics 44 174012
[30] Onclin S, Ravoo B J and Reinhoudt D N 2005 Engineering Silicon Oxide Surfaces Using Self-Assembled Monolayers Angewandte Chemie International Edition 44 6282-304
[31] Winesett D A, Story S, Luning J and Ade H 2003 Tuning Substrate Surface Energies for Blends of Polystyrene and Poly(methyl methacrylate) Langmuir 19 8526-35
[32] Peters R D, Yang X M, Kim T K and Nealey P F 2000 Wetting Behavior of Block Copolymers on Self-Assembled Films of Alkylchlorosiloxanes: Effect of Grafting Density Langmuir 16 9620-6
[33] Giammaria T J, Ferrarese Lupi F, Seguini G, Perego M, Vita F, Francescangeli O, Wenning B, Ober C K, Sparnacci K, Antonioli D, Gianotti V and Laus M 2016 Micrometer-Scale Ordering of Silicon-Containing Block Copolymer Thin Films via High-Temperature Thermal Treatments ACS Applied Materials & Interfaces 8 9897-908
[34] Borah D, Shaw M T, Holmes J D and Morris M A 2013 Sub-10 nm Feature Size PS-b-PDMS Block Copolymer Structures Fabricated by a Microwave-Assisted Solvothermal Process ACS Applied Materials & Interfaces 5 2004-12

[35] Borah D, Rasappa S, Senthamaraikannan R, Kosmala B, Shaw M T, Holmes J D and Morris M A 2012 Orientation and Alignment Control of Microphase-Separated PS-b-PDMS Substrate Patterns via Polymer Brush Chemistry ACS Applied Materials & Interfaces 5 88-97

[36] Borah D, Ozmen M, Rasappa S, Shaw M T, Holmes J D and Morris M A 2013 Molecularly Functionalized Silicon Substrates for Orientation Control of the Microphase Separation of PS-b-PMMA and PS-b-PDMS Block Copolymer Systems Langmuir 29 2809-20

[37] Fryer D S, Peters R D, Kim E J, Tomaszewski J E, de Pablo J J, Nealey P F, White C C and Wu W-l 2001 Dependence of the Glass Transition Temperature of Polymer Films on Interfacial Energy and Thickness Macromolecules 34 5627-34

[38] Hsieh I F, Sun H-J, Fu Q, Lotz B, Cavicchi K A and Cheng S Z D 2012 Phase structural formation and oscillation in polystyrene-block-polydimethylsiloxane thin films Soft Matter 8 7937-44

[39] Hanley K J, Lodge T P and Huang C I 2000 Phase behavior of a block copolymer in solvents of varying selectivity Macromolecules 33 5918-31

[40] Lodge T P, Pudil B and Hanley K J 2002 The full phase behavior for block copolymers in solvents of varying selectivity Macromolecules 35 4707-17

[41] Cheng S Z D 2008 Phase Transitions in Polymers: The Role of Metastable States Elsevier Science

[42] Rasappa S, Borah D, Senthamaraikannan R, Faulkner C C, Shaw M T, Gleeson P, Holmes J D and Morris M A 2012 Block copolymer lithography: Feature size control and extension by an over-etch technique Thin Solid Films 522 318-23

[43] Andreozzi A, Lamagna L, Seguini G, Fanciulli M, Schamm-Chardon S, Castro C and Perego M 2011 The fabrication of tunable nanoporous oxide surfaces by block copolymer lithography and atomic layer deposition Nanotechnology 22 335303

[44] Pellegrino P, Perego M, Schamm-Chardon S, Seguini G, Andreozzi A, Lupi F F, Castro C and Assayag G B 2013 Fabrication of well-ordered arrays of silicon nanocrystals using a block copolymer mask physica status solidi (a) 210 1477-84

[45] Girardot C, Böhme S, Archambault S, Salaün M, Latu-Romain E, Cunge G, Joubert O and Zelsmann M 2014 Pulsed Transfer Etching of PS–PDMS Block Copolymers Self-Assembled in 193 nm Lithography Stacks ACS Applied Materials & Interfaces 6 16276-82

[46] Archambault S, Girardot C, Salaün M, Delalande M, Böhme S, Cunge G, Pargon E, Joubert O and Zelsmann M 2014 Directed self-assembly of PS-*b*-PDMS into 193nm photoresist patterns and transfer into silicon by plasma etching. pp 90540O-O-8